available at www.sciencedirect.com

SCIENCE DIRECT®

journal homepage: www.ejconline.com

Establishment and characterization of xenografts and cancer cell cultures derived from *BRCA1* −/− epithelial ovarian cancers

Stefano Indraccolo[a,*], *Veronica Tisato*[b], *Simona Agata*[b], *Lidia Moserle*[b], *Silvia Ferrari*[b], *Monia Callegaro*[b], *Luca Persano*[b], *Maurizia Dalla Palma*[b], *Maria Chiara Scaini*[b], *Giovanni Esposito*[a], *Ambrogio Fassina*[c], *Ornella Nicoletto*[a], *Mario Plebani*[d], *Luigi Chieco-Bianchi*[b], *Alberto Amadori*[a,b], *Emma D'Andrea*[a,b], *Marco Montagna*[a]

[a]*Istituto Oncologico Veneto, Padova, Italy*
[b]*Section of Oncology, Department of Oncology and Surgical Sciences, University of Padova, Padova, Italy*
[c]*Section of Pathology and Cytopathology, Department of Oncology and Surgical Sciences, University of Padova, Padova, Italy*
[d]*Department of Laboratory Medicine, Medical and Surgical Sciences, University of Padova, Padova, Italy*

ARTICLE INFO

Article history:
Received 23 November 2005
Received in revised form
20 January 2006
Accepted 20 January 2006
Available online 8 June 2006

Keywords:
Ovarian cancer
BRCA1
Xenograft
CA125
MLPA

ABSTRACT

The *BRCA1* gene is responsible for a high number of hereditary breast and ovarian cancers that cluster in families with a strong genetic predisposition. Despite intense investigation, the accumulating findings on BRCA1 biological functions have not yet been translated into specific therapeutic approaches, also due to the lack of suitable experimental models. The purpose of this study was to establish and characterize cell cultures and xenografts from patients with *BRCA1* −/− ovarian cancers. We derived two ovarian cancer cell lines, termed PD-OVCA1 and PD-OVCA2, both from patients previously treated with chemotherapy, that propagate in SCID mice as well as *in vitro* for a limited number of passages. Both cell lines expressed cytokeratins and the CA125 tumour marker. A detailed molecular characterization highlighted both constitutive and somatic genetic events that abrogate *BRCA1* gene function. Both cell lines were shown to lose the wild type *BRCA1* allele; intriguingly, these deletions were apparently accompanied by gain of one or more copies of the mutant alleles. Finally, a genomic profile of major chromosomal aberrations was obtained by the Multiplex Ligation-dependent Probe Amplification (MLPA) technique, which disclosed chromosomal imbalances targeting specific genes in each cell line. The PD-OVCA1 and PD-OVCA2 ovarian cancer cell lines will provide a valuable tool for new experimental models for the study of BRCA1-associated tumour biology.

1. Introduction

Ovarian cancer is the leading cause of death from gynecologic cancer in the world and it is one of the most common forms of hereditary cancer in adult females.[1] Mendelian transmission of ovarian cancer predisposition includes cancer syndromes such as the Lynch Syndrome and the Hereditary Breast Ovarian Cancer Syndrome. The latter is linked to pathogenic mutations in the *BRCA1* or *BRCA2* genes which account for the majority of cases with an extensive cancer

* *Corresponding author:* Present address: Section of Oncology, Department of Oncology and Surgical Sciences, via Gattamelata, 64, University of Padova, I-35128 Padova, Italy. Tel.: +39 0498215875; fax: +39 0498072854.
E-mail address: stefano.indraccolo@unipd.it (S. Indraccolo).
0959-8049/$ - see front matter © 2006 Elsevier Ltd. All rights reserved.
doi:10.1016/j.ejca.2006.01.057

family history, with the *BRCA1* gene making the major contribution.[2] While precise estimates of *BRCA1* and *BRCA2* mutation penetrances are still the subject of considerable controversy, a recent meta-analysis of 22 population studies estimated a cumulative risk of ovarian cancer of 39% and 11% for *BRCA1* and *BRCA2* carriers respectively.[3]

A growing body of evidence suggests that BRCA1 protein is involved in the DNA repair response as well as in the maintenance of chromosomal stability.[4] Abnormal DNA repair mechanisms contribute to carcinogenesis and also modify the tumour's response to chemotherapy. Accordingly, loss of BRCA1 function is associated with increased sensitivity to DNA-damaging chemotherapy. Similar conclusions were reached by retrospective clinical studies investigating chemotherapy effectiveness in breast and/or ovarian cancer patients who carry BRCA1 mutations, thus suggesting that *BRCA1* gene status may represent a relevant predictive biomarker for clinical response to DNA-damaging agents (reviewed by Ref. [5]). Therefore, there is much interest in establishing xenografts and cell lines carrying mutations in the *BRCA1* gene as they could provide useful tools to investigate BRCA1 protein functions *in vitro* as well as in small animal models. Although many ovarian cancer cell lines have been described, they have been generally established *in vitro*, mostly from patients with sporadic epithelial ovarian cancer (EOC):[6–11] only one *BRCA1* negative ovarian cancer cell line, derived from a relatively rare endometrioid carcinoma, has been reported so far.[11] In order to avoid *in vitro* selection of tumour cells, which could result in the loss of some of the features of the primary tumour, we attempted to grow tumour cells in the peritoneal cavity of immunodeficient mice, and obtained tumour xenografts of ovarian cancer from patients with a hereditary *BRCA1* mutation. These xenografts are usually maintained through serial passages *in vivo*, and they can be cultivated as primary cultures for a limited number of passages. We report here the characterization of these primary cultures which we feel will be useful to study the molecular biology of hereditary ovarian cancer and to investigate novel therapeutic approaches.

2. Materials and methods

2.1. Patient information

CD, a 67-year-old white female underwent assessment laparotomy in July 2001, which disclosed peritoneal carcinomatosis of a grade 3, stage IV papillary serous ovarian carcinoma. Of note, the patient was previously treated for breast cancer with radical surgery followed by radiotherapy and chemotherapy with taxotere/doxorubicin. Ovarian cancer was diagnosed 8 months after the end of adjuvant chemotherapy. Postoperative chemotherapy consisted of 10 courses of carboplatin; a partial clinical response was measured in March 2002. However, in September 2002, the patient had a liver recurrence, which was treated with additional 4 courses carboplatin. In January 2003, the patient received gemcitabin and topotecan due to liver and lymph nodes disease progression and achieved a partial response. In May 2003, however, the patient developed abdominal ascites requiring paracentesis and was treated with mitoxantrone i.p. The patient died in August 2003, 25 months after the original diagnosis of Stage IV ovarian cancer.

The second patient, BMA, a 70-year-old white female was diagnosed with a grade 3, stage III papillary serous ovarian carcinoma and underwent cytoreductive surgery in April 2001. She was subsequently treated with carboplatin/taxol chemotherapy for 6 cycles. The patient remained in complete clinical remission until January 2004, when she developed a liver recurrence with ascites and increased CA125 serum levels. She was promptly treated with carboplatin/taxol and achieved a complete response. In March 2005, the patient developed an inguinal lymph node metastasis, which was surgically removed. She is currently alive and disease free.

Blood and ascitic fluid samples were obtained from patients after receiving their informed consent.

2.2. Establishment of the xenografts and primary cell lines

Ascitic fluid was obtained in May 2003 and January 2004 for patient CD and BMA, respectively, and, when observed at phase-contrast microscopy, it contained many large oval cells with prominent nuclei. Tumour cells were isolated from the neoplastic effusion by centrifugation at 500 g and resuspended in RPMI 1640 tissue culture medium (Euroclone, Milan, Italy). Approximately 3×10^6 tumour cells were injected i.p. into a 6-week old SCID mice (Charles River, Wilmington, MA, USA). Procedures involving animals and their care conformed with institutional guidelines that comply with national and international laws and policies (EEC Council Directive 86/609, OJ L 358, 12 December, 1987). About 2 months later, animals developed ascites and were sacrificed: autopsy revealed abundant haemorrhagic ascites and multiple solid tumours infiltrating the liver capsule and the diaphragm. The primary ovarian cancer cell lines PD-OVCA1 and PD-OVCA2 were derived from the malignant effusion of the mice injected with cells from patient CD and BMA, respectively. Ascites cells were centrifuged; red blood cells were lysed by ammonium chloride and the tumour cells were resuspended in RPMI 1640 supplemented with 10% v/v FCS, 2 mM L-glutamine, kanamicin (100 μg/ml) and cultivated in 25 cm^2 tissue culture flasks. At *in vitro* passage 2-3, when most of the tumour cells were viable and proliferating, some of the cultures were used to inoculate SCID mice i.p. (3×10^6 cells/mouse) in order to propagate the xenograft: secondary tumours developed slightly more quickly; the mice developed ascites and were sacrificed 40 days after tumour cell injection. Biological concordance between the *in vivo* tumour-derived cell lines and the corresponding patients was performed on DNA, extracted by phenol-chloroform procedures and analysed by means of the AmpFlSTR Profiler identity kit (Applied Biosystems) according to the conditions provided by the manufacturer.

At time of writing, PD-OVCA1 and PD-OVCA2 cells have been passed 15 and 8 times *in vivo*, respectively, fully maintaining their tumourigenicity. EBV-immortalized lymphoblastoid cell lines were established from peripheral blood lymphocytes of both patients according to standard procedures.[12]

2.3. Immunocytochemistry and immunohistochemistry

Immunocytochemistry studies were performed using avidin-biotin complex (ABC) kit (Vector Laboratories, Burlingame, CA) and a mouse streptavidin biotin complex (SABC) kit (BioGenex, San Ramon, CA). The anti-cytokeratin AE1/AE3 and the anti-vimentin antibodies were from BioGenex and were used at 1:100 dilution, the anti-desmin antibody was from Dako (Glostrup, Denmark) and was used at a 1:50 dilution. Tumours grown in mice were quickly frozen in liquid nitrogen after surgical removal and stored at −80 °C. Immunohistochemistry was performed on frozen sections after a 10' acetone fixation at 4 °C. The staining procedure was carried out with Ab-4 antibody diluted 1:50 for 1 hour at room temperature (mouse monoclonal, clone SD118) (Calbiochem, Cambridge, MA) using the ImmPRESS technique (ImmPRESS reagent kit, Vector Laboratories, Burlingame, CA) and 3-3′ diaminobenzidine (DAB kit, Dakocytomation, Glostrup, Denmark) as chromogen substrate. Finally, the sections were lightly counterstained with Mayer's haematoxylin. The specificity of the staining procedure was confirmed by replacing the primary antibody with phosphate buffered saline.

2.4. CA125 measurement

The concentration of CA125 in the conditioned supernatant of primary ovarian cancer cell cultures and in the sera of SCID mice injected i.p. with these cells was determined by the Bayer Advia Centaur analyzer (Diamond Diagnostics, Holliston, MA). Cells (1×10^6) were seeded into 25-cm^2 flasks in complete RPMI medium and the conditioned supernatant was harvested three days later and stored at −80 °C until assayed. Sera were collected from animals bearing advanced tumours, usually 1 month after tumour cell injection, and stocked at −80 °C until assayed.

2.5. BRCA1 mutational analysis

Constitutive as well as somatic (tumour-acquired) mutations were investigated by a combination of different mutation detection approaches. More specifically, germ-line point mutations were searched by screening all *BRCA1* exons and exon-intron boundaries by means of Denaturing High-Performance Liquid Chromatography (DHPLC); major genomic rearrangements of the *BRCA1* gene were evaluated by means of the recently described Multiple Ligation-dependent Probe Amplification (MLPA). The MLPA procedure was performed according to the manufacturer's instructions (MRC Holland, Amsterdam, the Netherlands) on a PTC 200 (MJ Research INC., Waltham, MA) thermal cycler using FAM-labelled primers. Variations in peak height were evaluated by comparing each sample with a normal control.

2.6. Loss of Heterozygosity (LOH) analysis

Deletion of the wild type allele in the ovarian cell lines was performed by typing the microsatellites D17S1855, D17S1322, D17S1323 and D17S1327. Each marker was independently PCR-amplified from the ovarian and lymphoblastoid cell lines using FAM-labelled forward primers. PCR products were analysed by capillary gel electrophoresis using the ABI Prism-310 Genetic Analyser (Applied Biosystems).

2.7. Expression of the BRCA1 mutant alleles

RNA was isolated from ovarian and lymphoblastoid cell lines using the RNAzol reagent (Tel-Test, Friendwood, TX), following manufacturer's instructions. RT-PCR analysis of *BRCA1* transcripts was carried out using the Superscript™ RT RnaseH⁻ reverse transcriptase (Invitrogen, Carlsbad, CA). Primer couples employed to amplify the mutant transcripts are available upon request. Sequence analysis of the mutant transcripts was performed with the DNA sequencing kit (Applied Biosystems) followed by capillary gel electrophoresis with the ABI Prism-310 Genetic Analyser (Applied Biosystems).

For the immunofluorescence experiments, cells were grown in 6 well plates onto glass coverslips (collagen I-coated for the PD-OVCA1 cell line). Living cells, cultured in RPMI (ovarian cancer cell lines) or DMEM (HeLa-tat and IGROV-1) medium supplemented with 10% v/v FBS and 2 mM L-glutamine, were washed twice with PBS and fixed in phosphate-buffered 3.7% v/v formaldehyde for 10 minutes, permeabilized with 0.2% v/v Triton X-100 in PBS for 10 minutes, and blocked with 3% w/v BSA for 30 minutes. Dual labelling immunofluorescence experiments were carried out by staining cells with Ab-1 antibody (1:80 dilution of the mouse monoclonal, clone MS110) (Calbiochem) for the BRCA1 protein and CRM1-specific antibody (1:200 dilution, kindly provided by Dr. M. Newmann). Primary antibodies were visualized by secondary antibodies Alexa Fluor 594 and 488 used at a 1:500 dilution (Molecular Probes). Laser-scanning microscopy was carried out with a Zeiss LSM 510 microscope (Carl Zeiss, Jena, Germany) using Argon (488 nm) and Helium-Neon (543 nm) lasers. Scan parameters such as laser intensity and pinhole aperture were standardized to allow comparison of signals obtained in different samples. Negative controls were obtained by omission of the primary antibody.

2.8. MLPA genomic profile

The SALSA human chromosomal aberration kits P005, P006, P007 (MRC-Holland, Amsterdam, the Netherlands) were employed for a genome-wide search for chromosomal aberrations in the conditions suggested by the manufacturer. Amplified samples were denatured and separated by capillary electrophoresis on an ABI 310 sequencer (Applied Biosystems). Probe specific signals were normalized by dividing each peak height for total height of that specific probe set. The resulting relative height was than compared to mean values of relative peak heights derived from normal female controls. Each sample was analysed in duplicate. Three different probes were excluded from the analysis as they gave inconsistent results.

3. Results

3.1. In vivo and in vitro features

Xenografts were established from malignant ascites of two patients with EOC. Grossly, the tumours grown in SCID mice

were partly solid with abundant haemorrhagic ascites (not shown). The appearance of the original tumours from the patients, the solid component of the tumours developed in SCID mice, and the microscopic features of the cultured cell lines PD-OVCA1 and PD-OVCA2 that we derived from the xenografts are shown in Fig. 1. Briefly, tumours in SCID mice consisted of invading nests of epithelial cells surrounded by fibrotic stroma, apparently more abundant in the case of PD-OVCA1 cells, with scarce evidence of inflammatory cell infiltration. *In vitro*, both cell lines grew initially in suspension forming floating spheroids with high cell viability (80–90%); in the case of PD-OVCA2 cells, some adherent nests were observed shortly after isolation from the animals. At later passages, usually passage 4–5, cells of both lines became prevalently adherent with progressive disappearance of the spheroids. Cell proliferation was very marked during the first 4–5 passages, as evaluated by the ViaLight ATP assay (Cambrex, Blatimore, MD), but slowed down thereafter and the cultures invariably stopped to proliferate and died by passage 6–7, usually 14–21 days after their recovery from the animals (data not shown). *In vitro*, PD-OVCA1 and PD-OVCA2 at passage number 3 released 558.5 U/ml and 1480.7 U/ml CA125, respectively. Moreover, sera from mice injected with PD-OVCA1 and PD-OVCA2 cells and with advanced signs of peritoneal carcinomatosis yielded 16.4–162.8 and 7.1–20.7 U/ml of CA125, respectively, indicating that tumour cells maintained production of the CA125 antigen also *in vivo*. Results concerning the expression of keratins and intermediate filaments are shown in Table 1. Both cell lines expressed keratins, revealed with mAb specific for high molecular weight chains (AE1 and AE3), confirming their epithelial origin. Among the intermediate filaments, vimentin was expressed by both cell lines, albeit with stronger reactivity in PD-OVCA2 compared to PD-OVCA1 cells, while desmin was negative or weakly expressed (Table 1). Interestingly, it has been demonstrated that coexpression of vimentin and cytokeratins is a peculiar feature of the ovarian surface epithelium and granulosa cells,[13] and it has also been observed in other EOC-derived cell lines.[6]

Table 1 – Expression of keratins and intermediate filaments by PD-OVCA1 and PD-OVCA2 cells

Antibody	PD-OVCA1	PD-OVCA2
AE1	++	++
AE3	+++	++
Vimentin	+	+++
Desmin	–	–/+

–, negative staining; –/+, positive staining of <25% of the cells; +, positive staining of 25–50% of the cells; ++, staining of 50–75% of the cells; +++, staining of >75% of the cells. AE1 and AE3 are high molecular weight cytokeratins of 40–56.5 kDa and 40–70 kDa, respectively.

3.2. *BRCA1* genotype analysis

While patient CD was affected by both breast and ovarian cancer and had a modest family history of both tumours, BMA developed an ovarian cancer and belongs to a family including at least two first-degree breast cancer cases. Both these features (i.e. breast and ovarian cancer in the same patient and presence of ovarian cancer in a family with multiple breast cancer cases) represent criteria that are strongly suggestive of a *BRCA1* mutation in our sample series.[14] Accordingly, patient BMA was find to carry a frameshift mutation (5083del19) whereas a genomic deletion removing *BRCA1* exon 17 was recently identified in patient CD during the search for major genomic rearrangements in a large number of breast and ovarian cancer families without detectable *BRCA1* and *BRCA2* point mutations (data not shown).

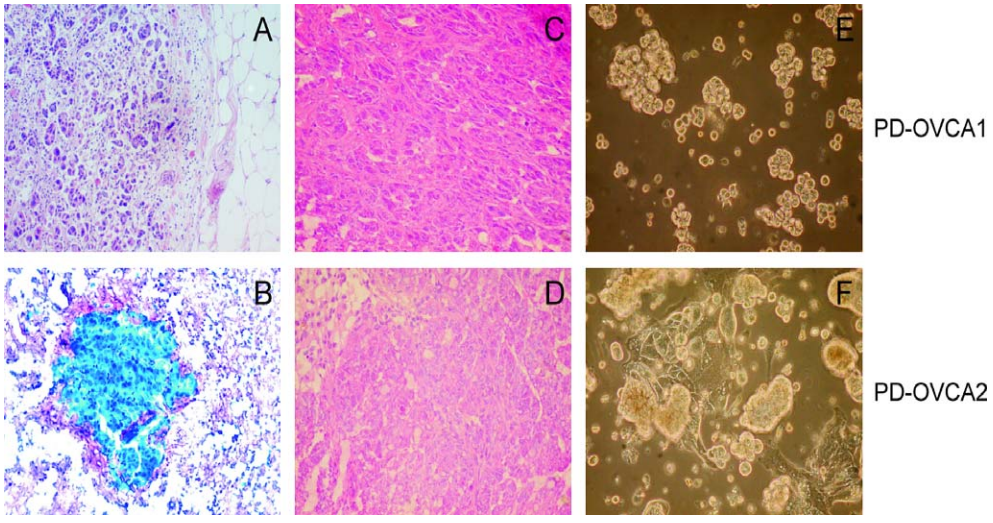

Fig. 1 – Morphology of the PD-OVCA1 and PD-OVCA2 cell lines. Histological preparations of the original tumours in the patients (panels A and B, representing an haematoxilin/eosin stain of a soft tissue and a Diff-Quik stain of an inguinal lymph node metastasis, respectively, 200x magnification), of the solid component of the xenograft tumours in SCID mice (panels C and D, 400x magnification) and phase-contrast photomicrographs of the cultured ovarian cancer cells PD-OVCA1 and PD-OVCA2 (panels E and F, 200x magnification).

Although generated by two different mechanisms, the two mutations cause premature termination codons at close aminoacid positions (1670 and 1672 in patients BMA and CD, respectively), thus likely exerting very similar pathogenic effects.

As a first step in the characterization of the *BRCA1* genotype in PD-OVCA1 and PD-OVCA2 cell lines, we used the MLPA technique to compare the profiles obtained from constitutive DNA, derived from the EBV-immortalized lymphoblasts, versus the *in vivo* derived ovarian cancer cell lines. The complete lack of the peak corresponding to exon 17 in PD-OVCA1 (Fig. 2) clearly indicated the loss of the wild-type allele. It is noteworthy that 4 out of the 10 control probes were associated with abnormally sized peaks. These probes recognize genes located on different chromosomes whose copy number variation likely reflects the cell line's genomic instability. A similar variability in control peaks was observed in the analysis of PD-OVCA2 (Fig. 2). In this case, however, the 19 nucleotides constitutive deletion did not perturb the annealing and ligation of the exon 16 specific probes, thus precluding the discrimination of mutant and wild type *BRCA1* alleles. Therefore, we decided to further investigate the allele loss by genotyping the four microsatellites D17S1855, D17S1322, D17S1323 and D17S1327 which mark the *BRCA1* locus. LOH for at least one marker was observed by comparison of the normal versus cell line derived DNA in both cases, confirming the deletion of one *BRCA1* allele (data not shown).

3.3. *Expression analysis of BRCA1 mutant alleles*

Using PCR primers located in the exons flanking those containing the germ-line mutations, we retro-amplified the *BRCA1* transcripts from RNA extracted from the two ovarian cancer cell lines. As shown in Fig. 3, only the band corresponding to the size of the mutant allele was present in the cell line PD-OVCA1. Similarly, the RT-PCR product obtained from the PD-OVCA2 cell line migrated slightly faster than the wild type allele, thus suggesting the expression of the 19 nucleotides deleted allele. Direct sequencing of these PCR fragments confirmed the selective expression of the mutant transcripts in both cases (data not shown).

In order to evaluate the mutant proteins' expression by immunofluorescence, cells derived from fresh *ex vivo* passages were plated onto coverslips. While a good proportion of the PD-OVCA2 cells adhered onto the coverslips, only a small fraction of the PD-OVCA1 cells attached to the support, even after collagen I treatment of the coverslips. Immunofluorescence staining was performed with the MS110 mouse monoclonal antibody that recognizes an epitope in the BRCA1 aminoterminal region which should be retained by both BRCA1 mutant proteins. HeLa -tat as well as IGROV-1 cell lines were used as positive controls, and showed the typical S-phase-specific dot-like staining of the BRCA1 protein (Fig. 4A). On the other hand, this was not observed in either of the two cell lines PD-OVCA1 and PD-OVCA2 (Fig. 4A), apparently suggesting a very low expression or mislocalization of the mutant proteins. To confirm these data, the anti-BRCA1 SD118 mouse monoclonal antibody, directed towards an exon 11 epitope, was used in immunohistochemistry on frozen sections from the xenografts grown in SCID mice. Similarly to what observed by immunofluorescence, a clearly positive signal was obtained in the IGROV-1-derived tumour whereas no BRCA1 signal was detectable in either of the two patient-derived tumours (Fig. 4B). Overall, these results indicate that

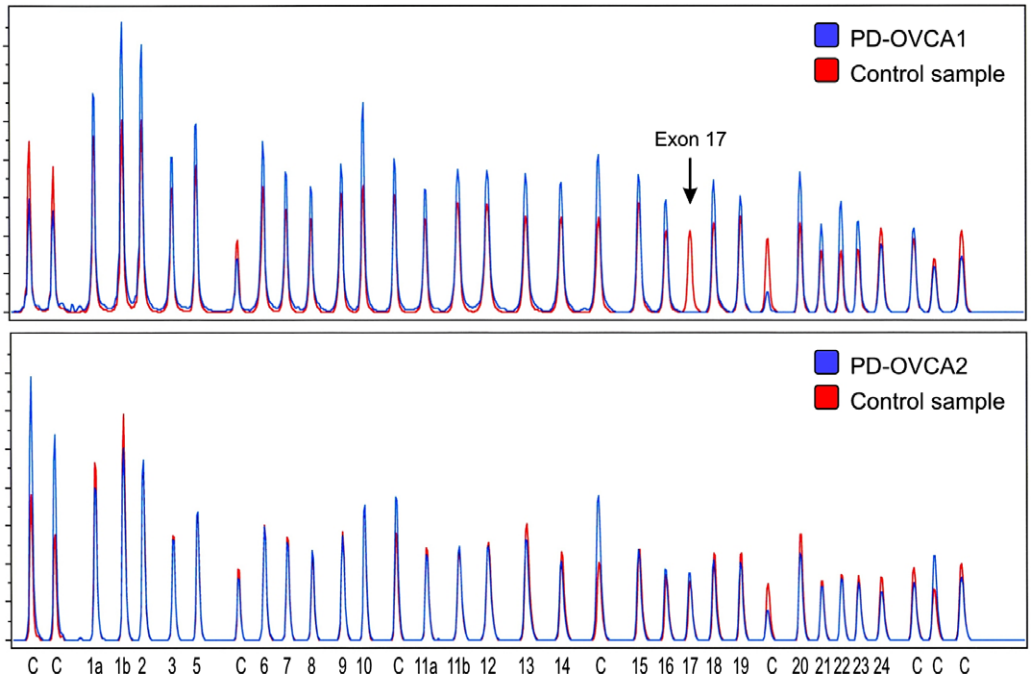

Fig. 2 – *BRCA1* MLPA profile in PD-OVCA1 and PD-OVCA2. Profiles corresponding to *BRCA1* exons (numbered at bottom figure) and control probes (indicated by C) are obtained by the overlap of a normal control sample (red line) with each cell line (blue line). The arrow indicates the absence of exon 17 in PD-OVCA1 DNA.

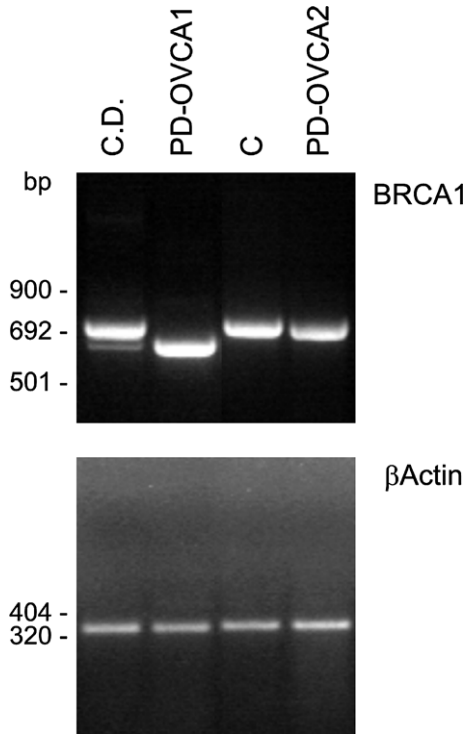

Fig. 3 – Analysis of *BRCA1* mutant transcripts. RT-PCR analysis of *BRCA1* transcripts (exons 15–20) and β-actin control gene in ovarian cancer cell lines (PD-OVCA1 and PD-OVCA2), lymphoblasts from patient CD and a normal control (C).

PD-OVCA 1 and PD-OVCA2 cells lack detectable *BRCA1* expression.

3.4. *MLPA genomic profile*

In order to evaluate the type and number of chromosomal aberrations that occurred in the two cell lines, metaphases from proliferating cells were screened to define the specific alterations. Both cell lines displayed a very complex karyotype, making assignment of single chromosomes impractical as well as useless (data not shown). Therefore, the location of genomic regions disrupted during tumourigenesis or cell line establishment, were mapped by the MLPA technique using a combination of multiple probes recognizing 107 genes and one sequence tag located on different chromosomes.[15]

Normalized ratios for each of the 117 sequence-specific probes are reported in Fig. 5 as a percentage of change versus the normal female controls' mean value (cut-offs were arbitrarily set at more than 35% signal decrease for deletions and more than 30% signal increase for gains). A total number of 42 probes were shown to be represented in anomalous amounts in PD-OVCA2 and PD-OVCA1 likely reflecting a high degree of genomic instability (Fig. 5). The vast majority of the aberrations fell within chromosomal regions commonly altered in EOC (Mitelman Database of Chromosome Aberrations in Cancer: http://cgap.nci.nih.gov/Chromosomes/Mitelman) and/or ovarian cancer cell lines.[16] Notably, a few of these aberrations involved only one or two contiguous probes thus possibly identifying discrete minimal regions of alteration. For instance, while the cell line PD-OVCA2 shows a pretty large region of increased signal at 3q, only two contiguous probes result in a higher signal in PD-OVCA1. Significantly, the signal corresponding to the IL12A probe largely overcomes that of the adjacent MME probe, thus pointing out to a specific sub-region likely to represent the true target of the 3q amplification. A total absence of signal was observed for probes recognizing the *CDKN2A* and *CDKN2B* genes in cell line PD-OVCA2. Homozygous deletions of this chromosomal region are rather common in specific tumour types.[17] Using the CDKN2A/2B MLPA kit, the deletion breakpoints were located between *MLLT3* and *INFB1* genes at the telomeric site and TEK and ELAVL2 probes at the centromeric site (data not shown), thus suggesting a biallelic deletion of a 2.7–6.7 Mb region including some other 42 genes.

Among all probes generating anomalous signals, nearly half identified chromosomal sites subjected to the same type of alterations in both cell lines. While most of them coincided with common imbalances identified in ovarian carcinomas, a few (deletion of B2M probe at 15q21-q22 and gain for IL18 at 11q22.2-q22.3) were concordant with chromosomal alterations previously defined as specific to hereditary tumours.[18]

Alterations involving loci harbouring genes known to play a role in ovarian cancer tumourigenesis were identified in both cell lines. Among the most relevant, signal losses in PD-OVCA1 involved *TP53*, *CDH1* and *PTEN*. Surprisingly, the *BRCA1* gene was apparently duplicated, suggesting the presence of multiple copies of the mutant allele. Higher than normal signals in the same cell line also included the *myc* oncogene, which is frequently amplified in ovarian cancer, as well as *FGF3* (*INT2* proto-oncogene) and *CCND1* genes, which are located within the same chromosomal region. Unexpectedly, the *PIK3CA* gene, recently suggested as a potential oncogene frequently amplified in ovarian cancers,[19] was excluded from the minimal amplified region at 3q25-q26. While this finding might simply suggest the presence of multiple oncogenes targeted by this chromosomal aberration, exclusion of PIK3CA from the over-expressed genes might be counterbalanced by a "synonymous" genetic event represented by the loss of its negative regulator PTEN likely resulting in an analogous effect on the same signal transduction pathway. In the PD-OVCA2 cell line, potentially relevant gene alterations were those causing copy number reductions of the *CDKN2A* (see above) and *BRCA2* loci. The highest signal increase was associated with *RENT2* gene probe consistent with multiple copies of the genomic region containing this gene. The apparently normal level *BRCA1*-specific signal was likely the result of duplication of the mutant allele.

4. Discussion

In order to establish an *in vivo* model for the study of *BRCA1* −/− ovarian tumour, we derived two independent cell lines grown in SCID mice. Primary cultures from both PD-OVCA1 and PD-OVCA2 xenografts initially contained abundant spheroid-like structures (see Fig. 1), which have often been associated with the presence of cancer stem cells (reviewed by Ref. [20]). Intriguingly, a recent report identified similar growth features in primary ovarian cancer cultures from a sporadic EOC.[21] Thus, following optimization of *in vitro* culture conditions in

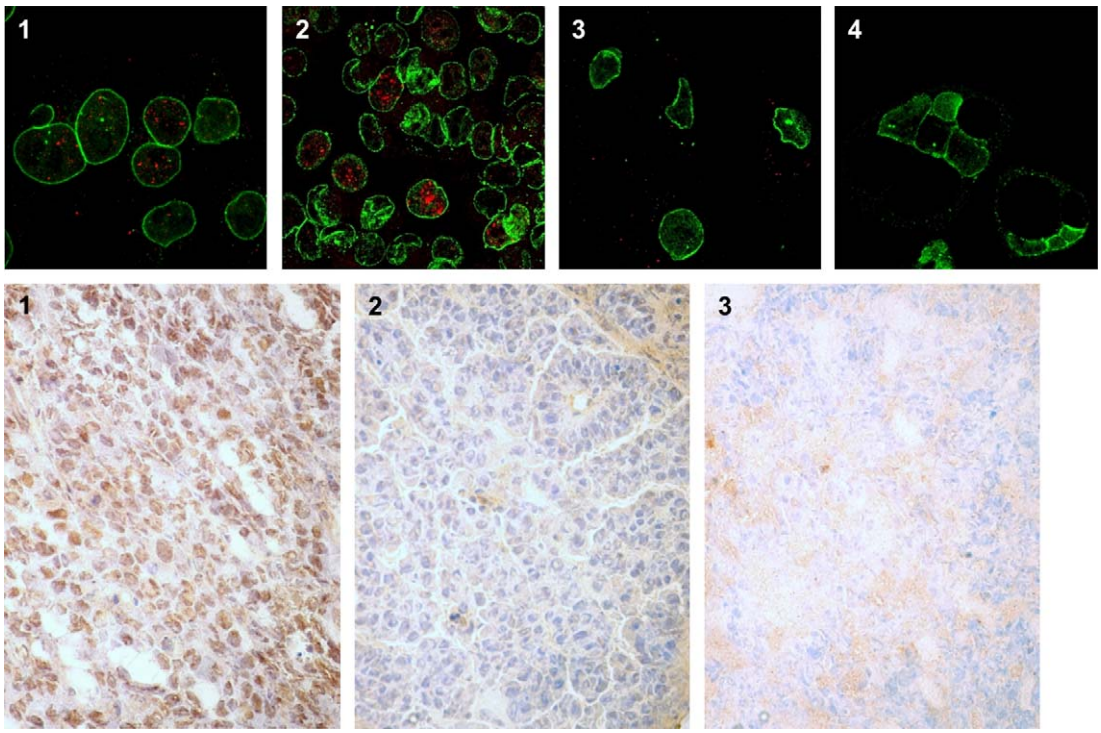

Fig. 4 – Immunofluorescence and immunohistochemistry analysis of BRCA1 mutant proteins. A) Immunofluorescent detection of BRCA1 protein (red) and nuclear membrane-specific CRM1 protein (green) in Hela-tat (1), IGROV-1 (2), PD-OVCA2 (3) and PD-OVCA1 (4). Slides were photographed at 600X magnification. B) Immunohistochemical BRCA1 staining of frozen tissue specimens from SCID mice tumours generated by inoculation of IGROV-1 (1), PD-OVCA1 (2) and PD-OVCA2 (3). Photographs at 400X magnification.

order to preserve these structures, PD-OVCA1 and PD-OVCA2 cultures could be potentially useful to investigate the possible existence and the features of *BRCA1* −/− ovarian cancer stem cells.

Functional inactivation of the *BRCA1* gene was demonstrated by a detailed characterization of both *BRCA1* alleles. Exon 17 deletion and 5083del19 germ-line mutations have an unambiguous pathogenic effect and cause premature protein termination. While the 5083del19 is one of the most recurrent mutations in Italy and likely originated in the South of the Country,[22] the exon 17 deletion was identified in four independent North-Italian breast and/or ovarian cancer families (Ref. [23] and data not shown). Both mutations disrupt one of the best characterized BRCA1 domains known as BRCT (for BRCA1 C-terminus). A specific biological role has been recently assigned to the BRCT motif which is also present in a large number of proteins mainly involved in DNA damage check point control and DNA repair.[24,25] According to the latest studies, the BRCT domain is a phosphopeptide binding motif able to discriminate the phosphorylation status of its protein partners. [26,27]

Using a combination of LOH and *BRCA1*-specific MLPA analyses, we demonstrated that the wild-type alleles are lost in both cell lines. Nonetheless, the genome-wide search for major genomic changes disclosed a normal (PD-OVCA2) or higher (PD-OVCA1) copy number of the chromosomal regions 17q21-q25 where the *BRCA1* gene is located. This finding is in line with a previous report[28] and may support the hypothesis of a direct involvement of multiple mutant alleles in the oncogenic process. In keeping with the genotypic data, *BRCA1* transcript analysis showed the selective presence of the mutant transcripts. Although we could not find evidence of BRCA1 mutant proteins either by immunofluorescence experiments or by immunohistochemistry on the tumours generated in SCID mice, we cannot exclude that the mutant variants are mis-located within the cell and/or their lack of expression reflects specific cell-cycle stages of the cells analysed. Whatever the case, on the basis of the structural alterations introduced by the mutations, as well as of the severe clinical phenotypes associated with inheritance of these mutations in breast and/or ovarian cancer families, we can conclude that both cell lines are null for a wild-type BRCA1 function.

The analysis of genome-wide chromosomal aberrations by the MLPA technique revealed multiple genomic imbalances in PD-OVCA1 and PD-OVCA2 reflecting a high-degree of genomic instability. These findings are in line with previous reports on BRCA1-associated breast and ovarian tumours and are consistent with the involvement of the BRCA1 protein in the DNA repair response. Most of the chromosomal alterations identified in the cell lines correspond to regions of frequent imbalances in ovarian carcinogenesis, thus suggesting that, despite of the high degree of genomic instability, the pathogenesis of sporadic and hereditary *BRCA1*-associated tumours involves similar genetic changes. On the other hand, since both patients have been treated with chemotherapeutics at the time

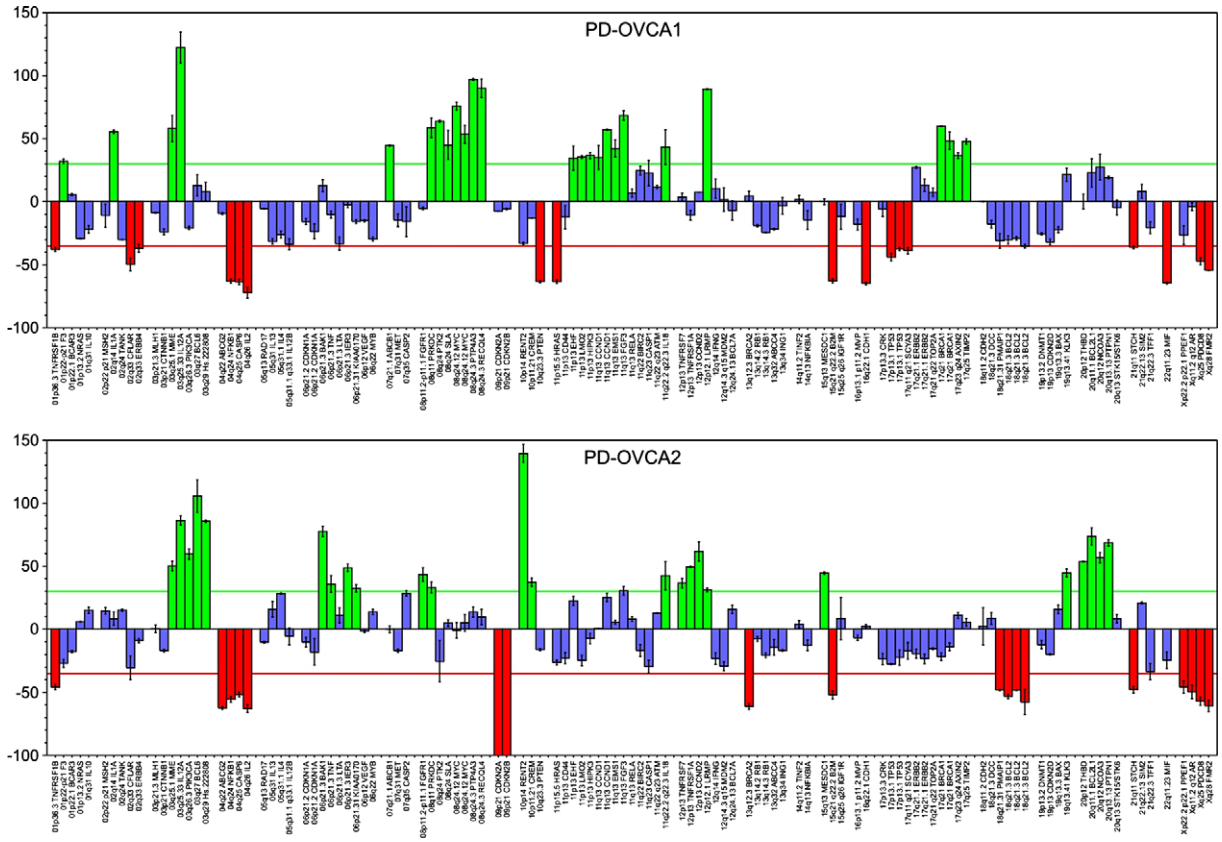

Fig. 5 – Graphical representation of the genomic imbalances in PD-OVCA1 and PD-OVCA2. Green bars indicate gains and red bar losses. Cut off values are shown by horizontal colored lines. Intensity values are expressed as percentage of variation versus a normal control mean value.

of establishment of the xenograft, we cannot exclude that some of the genomic changes could be treatment related. Homozygous deletions were observed only in PD-OVCA2 cell line at 9p21 and involved the *CDKN2A/B* loci coding for p16, p14 and p15 tumour suppressors. Deletions at this chromosomal region occur frequently in ovarian cancers[29] and in a number of other tumour types[17] likely reflecting the involvement of additional genes or the presence of alternative mutation mechanisms. [30] Indeed, while a role for p16 inactivation has been suggested in the pathogenesis of ovarian cancers and a correlation as also been established as a prognostic parameter,[31] whether *CDKN2A/B* loci are the only target of the chromosomal deletions remains to be determined. Using MLPA, chromosome 9p specific probes to further investigate the deleted alleles we demonstrated the homozygous loss of a several megabase-region containing a number of additional genes. Copy number changes were detected at many other chromosomal locations with a slightly different pattern in the two cell lines and involved relevant genes playing a role in ovarian carcinomas. Additional cancer related genes were found to be present in anomalous dosage. While most of these changes are likely to be relevant for the ovarian carcinogenesis process, the unequivocal definition of their causal role would need further supporting evidence. Nonetheless we provide a sort of "oncogenomic profile" that might be useful and instrumental to the design of specific studies of the BRCA1 protein on different genetic backgrounds.

In summary, we derived ovarian cancer xenografts and cell lines from patients affected by hereditary *BRCA1*-associated ovarian cancers. We provide sound evidence of the functional inactivation of the *BRCA1* gene as well as a gene-specific chromosomal aberration map. As the two cell lines were derived *in vivo* from treated patients we speculate that they might preserve bio-pathological features close to the original tumours and therefore represent a valuable tool as experimental models for the study of *BRCA1*-associated tumour biology as well as for studying genes involved in resistance to chemotherapeutics.

Conflict of interest statement

None declared.

Acknowledgements

We thank D. Zullato for her expert technical assistance, P. Gallo and A. Azzalini for artwork, and E. Piovan for help in preparing the manuscript. This work was supported by MIUR 40% and 60%, FIRB 2001, PRIN 2003, the Italian Association for Cancer Research (AIRC), the Ministero della Salute – Ricerca Finalizzata 2002, the Italian Foundation for Cancer Research (FIRC), Lega Italiana per la lotta contro i Tumouri (LILT) and the Fondazione Cassa di Risparmio di Padova e Rovigo.

REFERENCES

1. Risch HA, McLaughlin JR, Cole DE, et al. Prevalence and penetrance of germline BRCA1 and BRCA2 mutations in a population series of 649 women with ovarian cancer. *Am J Hum Genet* 2001;**68**(3):700–10.
2. Gayther SA, Russell P, Harrington P, Antoniou AC, Easton DF, Ponder BA. The contribution of germline BRCA1 and BRCA2 mutations to familial ovarian cancer: no evidence for other ovarian cancer-susceptibility genes. *Am J Hum Genet* 1999;**65**(4):1021–9.
3. Antoniou A, Pharoah PD, Narod S, et al. Average risks of breast and ovarian cancer associated with BRCA1 or BRCA2 mutations detected in case Series unselected for family history: a combined analysis of 22 studies. *Am J Hum Genet* 2003;**72**(5):1117–30.
4. Yoshida K, Miki Y. Role of BRCA1 and BRCA2 as regulators of DNA repair, transcription, and cell cycle in response to DNA damage. *Cancer Sci* 2004;**95**(11):866–71.
5. Kennedy RD, Quinn JE, Mullan PB, Johnston PG, Harkin DP. The role of BRCA1 in the cellular response to chemotherapy. *J Natl Cancer Inst* 2004;**96**(22):1659–68.
6. Alama A, Barbieri F, Favre A, et al. Establishment and characterization of three new cell lines derived from the ascites of human ovarian carcinomas. *Gynecol Oncol* 1996;**62**(1):82–8.
7. Gamboa G, Carpenter PM, Podnos YD, et al. Characterization and development of UCI 107, a primary human ovarian carcinoma cell line. *Gynecol Oncol* 1995;**58**(3):336–43.
8. Han X, Papadopoulos AJ, Jones TA, Sheer D, Raju KS. SR8–the establishment and characterisation of a new ovarian carcinoma cell line and xenograft model. *Eur J Cancer* 1996;**32A**(1):160–7.
9. Langdon SP, Lawrie SS, Hay FG, et al. Characterization and properties of nine human ovarian adenocarcinoma cell lines. *Cancer Res* 1988;**48**(21):6166–72.
10. Verschraegen CF, Hu W, Du Y, et al. Establishment and characterization of cancer cell cultures and xenografts derived from primary or metastatic Mullerian cancers. *Clin Cancer Res* 2003;**9**(2):845–52.
11. Yuan Y, Kim WH, Han HS, et al. Establishment and characterization of human ovarian carcinoma cell lines. *Gynecol Oncol* 1997;**66**(3):378–87.
12. Piovan E, Bonaldi L, Indraccolo S, et al. Tumour outgrowth in peripheral blood mononuclear cell-injected SCID mice is not associated with early Epstein-Barr virus reactivation. *Leukaemia* 2003;**17**(8):1643–9.
13. Santini D, Ceccarelli C, Mazzoleni G, Pasquinelli G, Jasonni GN, Martinelli GN. Demonstration of cytokeratin intermediate filaments in oocytes of the developing and adult human ovary. *Histochemistry* 1993;**99**(4):311–9.
14. Marroni F, Aretini P, D'Andrea E, et al. Evaluation of widely used models for predicting BRCA1 and BRCA2 mutations. *J Med Genet* 2004;**41**(4):278–85.
15. Worsham MJ, Pals G, Schouten JP, et al. Delineating genetic pathways of disease progression in head and neck squamous cell carcinoma. *Arch Otolaryngol Head Neck Surg* 2003;**129**(7):702–8.
16. Lambros MB, Fiegler H, Jones A, et al. Analysis of ovarian cancer cell lines using array-based comparative genomic hybridization. *J Pathol* 2005;**205**(1):29–40.
17. Ruas M, Peters G. The p16INK4a/CDKN2A tumour suppressor and its relatives. *Biochim Biophys Acta* 1998;**1378**(2):F115–77.
18. Zweemer RP, Ryan A, Snijders AM, et al. Comparative genomic hybridization of microdissected familial ovarian carcinoma: two deleted regions on chromosome 15q not previously identified in sporadic ovarian carcinoma. *Lab Invest* 2001;**81**(10):1363–70.
19. Shayesteh L, Lu Y, Kuo WL, et al. PIK3CA is implicated as an oncogene in ovarian cancer. *Nat Genet* 1999;**21**(1):99–102.
20. Pardal R, Clarke MF, Morrison SJ. Applying the principles of stem-cell biology to cancer. *Nat Rev Cancer* 2003;**3**(12):895–902.
21. Bapat SA, Mali AM, Koppikar CB, Kurrey NK. Stem and progenitor-like cells contribute to the aggressive behavior of human epithelial ovarian cancer. *Cancer Res* 2005;**65**(8):3025–9.
22. Baudi F, Quaresima B, Grandinetti C, et al. Evidence of a founder mutation of BRCA1 in a highly homogeneous population from southern Italy with breast/ovarian cancer. *Hum Mutat* 2001;**18**(2):163–4.
23. Montagna M, Santacatterina M, Torri A, et al. Identification of a 3 kb Alu-mediated BRCA1 gene rearrangement in two breast/ovarian cancer families. *Oncogene* 1999;**18**(28):4160–5.
24. Bork P, Hofmann K, Bucher P, Neuwald AF, Altschul SF, Koonin EV. A superfamily of conserved domains in DNA damage-responsive cell cycle checkpoint proteins. *Faseb J* 1997;**11**(1):68–76.
25. Callebaut I, Mornon JP. From BRCA1 to RAP1: a widespread BRCT module closely associated with DNA repair. *FEBS Lett* 1997;**400**(1):25–30.
26. Yu X, Chini CC, He M, Mer G, Chen J. The BRCT domain is a phospho-protein binding domain. *Science* 2003;**302**(5645):639–42.
27. Manke IA, Lowery DM, Nguyen A, Yaffe MB. BRCT repeats as phosphopeptide-binding modules involved in protein targeting. *Science* 2003;**302**(5645):636–9.
28. Staff S, Nupponen NN, Borg A, Isola JJ, Tanner MM. Multiple copies of mutant BRCA1 and BRCA2 alleles in breast tumours from germ-line mutation carriers. *Genes Chromosomes Cancer* 2000;**28**(4):432–42.
29. Niederacher D, Yan HY, An HX, Bender HG, Beckmann MW. CDKN2A gene inactivation in epithelial sporadic ovarian cancer. *Br J Cancer* 1999;**80**(12):1920–6.
30. Raschke S, Balz V, Efferth T, Schulz WA, Florl AR. Homozygous deletions of CDKN2A caused by alternative mechanisms in various human cancer cell lines. *Genes Chromosomes Cancer* 2005;**42**(1):58–67.
31. Kudoh K, Ichikawa Y, Yoshida S, et al. Inactivation of p16/CDKN2 and p15/MTS2 is associated with prognosis and response to chemotherapy in ovarian cancer. *Int J Cancer* 2002;**99**(4):579–82.